

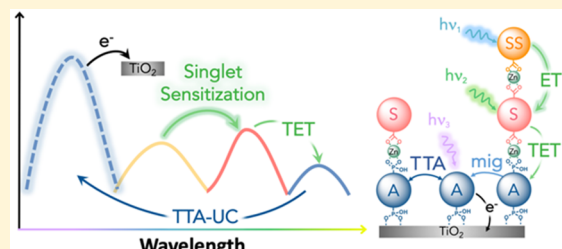
Singlet Sensitization-Enhanced Upconversion Solar Cells via Self-Assembled Trilayers

Yan Zhou,[‡] Cory Ruchlin,[‡] Alex J. Robb, and Kenneth Hanson*[‡]

Department of Chemistry & Biochemistry, Florida State University, Tallahassee, Florida 32306, United States

Supporting Information

ABSTRACT: Photon upconversion via triplet–triplet annihilation (TTA-UC) is a promising strategy for increasing maximum theoretical solar cell efficiencies by a factor of 1.3. However, one factor limiting integrated TTA-UC solar cell performance is the transmission window between sensitizer and acceptor molecule absorption. Here we demonstrate that the incorporation of a singlet sensitizer (SS) into a self-assembled trilayer is an effective means of harnessing that previously transmitted light. A record TTA-UC photocurrent density of 0.315 mA cm^{-2} under 1 sun irradiation was achieved and is attributed to directional SS-to-sensitizer singlet energy transfer and sensitizer-to-acceptor triplet energy transfer, followed by TTA, excited-state electron transfer into TiO_2 , and regeneration by a redox mediator in solution. These results demonstrate that singlet sensitization-enhanced self-assembled trilayers are a promising strategy for enhancing broad-band light absorption and improving the performance of TTA-UC solar cells.



Natural photosynthetic systems have evolved supramolecular assemblies with intermolecular orientations and distances that optimize the direction, rate, and efficiency of energy and electron transfer.¹ For manufactured devices like sensors, photodetectors, and photovoltaics, there is increasing interest in generating metal–organic frameworks,² dendrimers,³ multilayer assemblies,^{4–6} and other structures^{7,8} to realize similar levels of static and dynamic control. These human-made structures are not necessarily as well-defined or efficient as natural systems, at least not yet, but have the distinct advantage of enabling non-natural processes like photon upconversion via triplet triplet annihilation (TTA-UC),^{9,10} the process of combining two low-energy photons to generate a higher-energy excited state.^{11,12} TTA-UC can increase the theoretical efficiency of a single-junction solar cell from 33% to >43% by harnessing previously transmitted, sub-band gap light.^{13,14}

While there are several strategies for harnessing sunlight using TTA-UC,^{15–23} metal ion linked, multilayer assemblies of acceptor (aka, annihilator) (A) and triplet sensitizer (S) molecules on TiO_2 (Figure 1) have emerged as one of the most promising approaches for directly integrating TTA-UC into a solar cell.^{24–28} The layered structure enables directional energy transfer,²⁹ the molecular proximity is favorable for energy migration and TTA,^{30,31} and the metal oxide surface can extract charge from the UC state resulting in TTA-UC photocurrent density of up to 0.158 mA cm^{-2} under 1 sun (AM1.5).³² This photocurrent density enhancement is above the device relevant threshold of 0.1 mA cm^{-2} ,²¹ but given previously reported TTA-UC efficiencies, >1 mA cm^{-2} is most

certainly attainable and could increase device efficiency records for DSSCs or perovskite solar cells by one percentage point or more.³³ One factor limiting the performance of multilayer TTA-UC films is the absorption transparency window between A and S. Recently, Meinardi and co-workers overcame this shortcoming by incorporating a singlet sensitizer (SS) that absorbs in the transparency region and transfers energy to the triplet sensitizer, increasing TTA-UC emission quantum yield by a factor of 1.2.³⁴

Here we incorporate an SS into a TTA-UC solar cell as the third component of the self-assembled trilayers on TiO_2 (Figure 1). The SS harvests photons in the S-A transmission window, initiating an SS-to-S-to-A energy-transfer cascade followed by TTA-UC and charge extraction from the upconverted state. This co-operative scaffolding results in a TTA-UC photocurrent density of 0.314 mA cm^{-2} under 1 sun irradiation, a 2-fold increase on the previous record.

Fluorescein (SS in Figure 1) was selected as the singlet sensitizer because it has a carboxyl metal ion binding group and a ~90% fluorescence quantum yield (Table S3), and its absorption (425–525 nm) matches the S-A transmission window (Figure 2b). The trilayer film depicted in Figure 1 was prepared using a stepwise soaking procedure^{27,35} by submerging TiO_2 in a solution of A, then Zn^{II} , then S, then Zn^{II} again, and finally SS (Figure 2a). Each step of the surface modification procedure was monitored by absorption spec-

Received: April 23, 2019

Accepted: May 30, 2019

Published: May 30, 2019

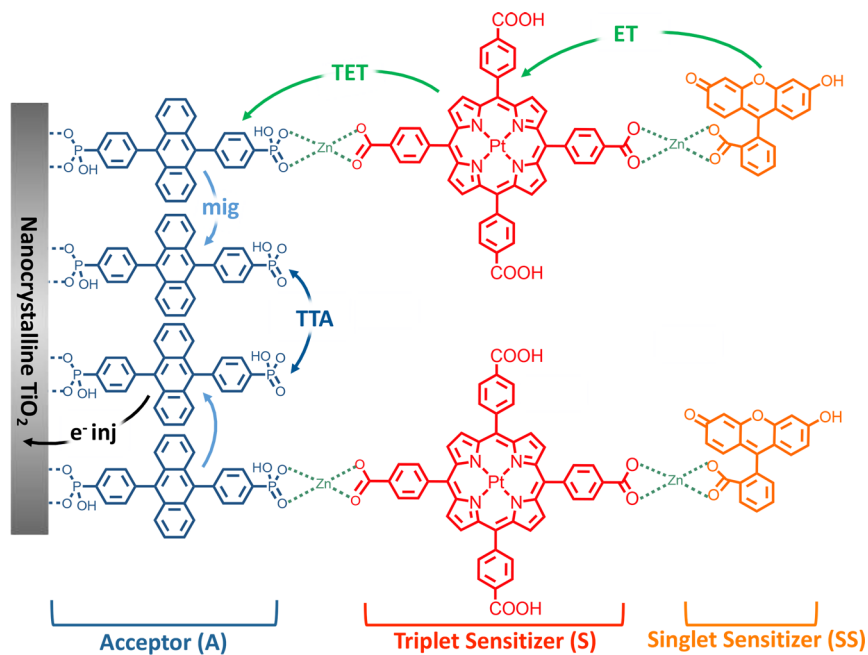


Figure 1. Schematic representation of self-assembled trilayer ($\text{TiO}_2\text{-A-Zn-S-Zn-SS}$) (ET = singlet energy transfer; TET = triplet energy transfer; mig = triplet exciton migration; TTA = triplet–triplet annihilation; e^- inj = electron injection).

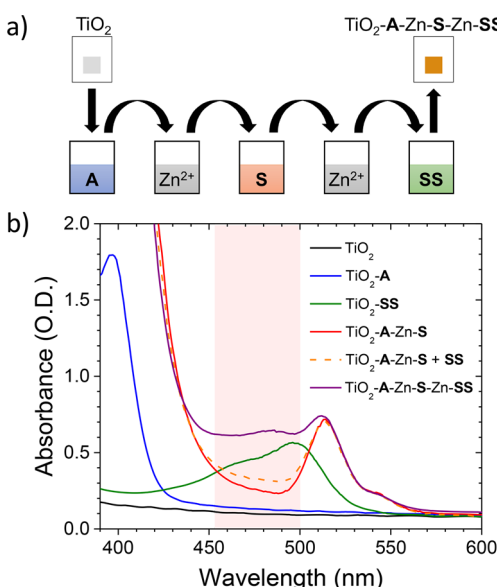


Figure 2. (a) Stepwise soaking procedure and (b) absorption spectra for the trilayer, bilayer ($\text{TiO}_2\text{-A-Zn-S}$), and constituent dyes on TiO_2 . The S-A transparency window is highlighted in pink.

troscopy (Figure 2b), and the fully loaded film has an A:S:SS ratio of 3:1:0.1 (details in [Experimental Methods](#)). It is important to note that although the structural details for the film are not known (i.e., molecular orientation), the absence of the second Zn^{II} treatment yet results in minimal contribution from SS absorption ($\text{TiO}_2\text{-A-Zn-S} + \text{SS}$ in Figure 2b), indicating that it forms a trilayer and not simply an SS + S codeposited layer. It is also worth noting that there was no change in the absorption spectra for $\text{TiO}_2\text{-A-Zn-S}$ before and after the second Zn^{II} treatment (Figure S2), indicating that there was most likely no dramatic change in the structure of the bilayer film (i.e., no aggregation or coordinate network formation).

Singlet-sensitized TTA-UC solar cells were fabricated with $\text{TiO}_2\text{-A-Zn-S-Zn-SS}$ as the photoanode, platinum as the counter electrode, and 0.2 M/0.02 M $\text{Co}^{\text{II}}/\text{Co}^{\text{III}}$ tris(1,10-phenanthroline) redox mediator in MeCN.³² $J_{\text{sc}}-t$ (short-circuit photocurrent density vs time) measurements of the B-SS, A-S bilayer, and A-S-SS trilayer devices under a simulated solar spectrum passed through a 455 nm long-pass filter, to isolate the contribution from TTA-UC, can be seen in Figure 3a. Triphenyl-4,4'-diphosphonic acid (B)³⁶ was used as a photo- and electrochemically inert surrogate in B-SS to retain the multilayer structure without the concerns of competitive energy or electron transfer.

As can be seen in Figure 3a, there is a nearly 2-fold increase in J_{sc} for A-S-SS trilayer relative to A-S bilayer device. Additionally, the incident photon-to-current efficiency spectra (IPCE) of both devices (Figure 3b) closely resemble their respective absorptance spectra but with a 3-fold enhancement in IPCE from 440 to 530 nm for the A-S-SS trilayer relative to A-S bilayer device (Figure S3). Equally important is that the trilayer J_{sc} is more than 10 times greater than that of B-SS or SS control (Figure S4), indicating that direct injection from SS into TiO_2 is negligible and is not responsible for the improved performance.

To gain further insights into the photocurrent generation mechanism, J_{sc} was measured with respect to 532 and 455 nm excitation intensity (Figure 3c) for the A-S and A-S-SS trilayer devices, respectively. Both films exhibit quadratic to linear intensity dependence, which is a characteristic feature of TTA-UC.^{37,38} For the trilayer, this observation directly supports involvement of singlet sensitizer excitation in the photon-to-current pathway via TTA-UC, again ruling out direct electron injection from SS. In terms of excitation events per second (excitation intensity \times absorptance), the crossover intensity between the two regimes (i.e., I_{th} value or the minimum excitation intensity for TTA-UC to reach maximum efficiency) for A-S-SS (1.3×10^{-15} excitation $\text{s}^{-1} \text{cm}^{-2}$) is nearly 2-fold lower than for A-S (2.1×10^{-15} excitation $\text{s}^{-1} \text{cm}^{-2}$). Both

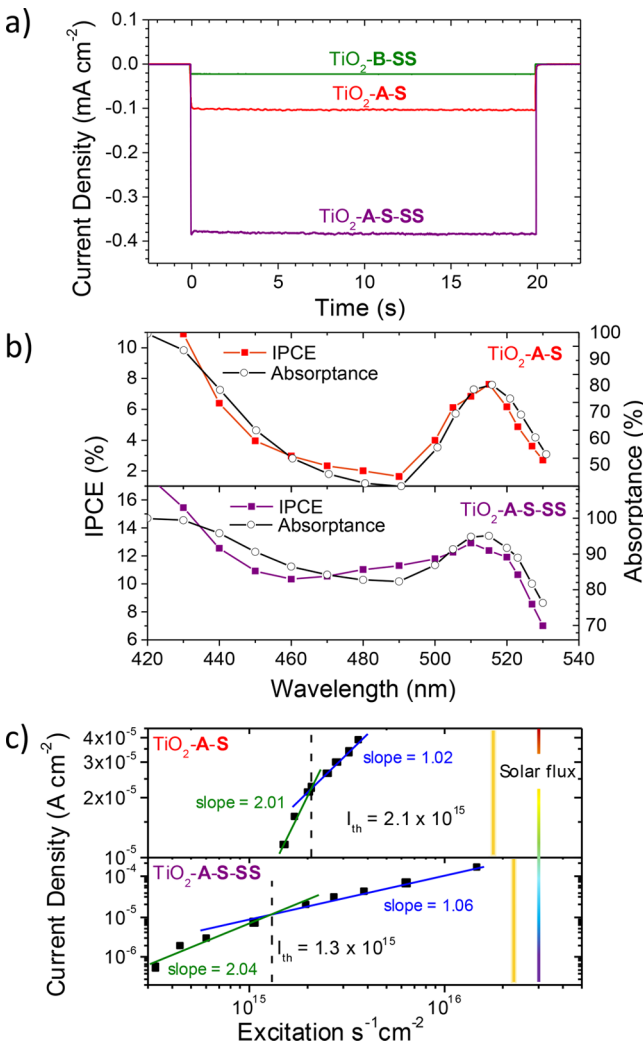


Figure 3. (a) Amperometric i - t curves under 1.15 equiv AM 1.5 solar irradiation passed through a 455 nm long-pass filter ($V = 0$ V; shutter open at $t = 0$ s, shutter closed at $t = 20$ s). (b) IPCE and absorptance spectra for bilayer and trilayer solar cells. (c) Photocurrent density at 0 V with respect to 532 and 455 nm laser intensity for the bilayer and trilayer, respectively.

crossover points are achieved well below AM 1.5 solar flux integrated from 455 to 535 nm (3.12×10^{-16} excitation s^{-1} cm^{-2} assuming 100% absorptance) and still below that even after correcting for the actual absorptance of the films (orange lines in Figure 3c). These results indicate that the $314 \pm 24 \mu A$ cm^{-2} for the trilayer film under 455 nm long-pass filtered AM 1.5 solar irradiation (Figure S5) is due to TTA-UC and is the highest photocurrent density yet achieved for a TTA-UC solar cell.

The proposed mechanism for the singlet-sensitized TTA-UC solar cell is depicted in Figure 4 with select productive and nonproductive processes highlighted in green and red, respectively. Briefly, excitation of SS ($k_{ex(SS)}$) is followed by SS to S singlet energy transfer (k_{ET_1}). The heavy Pt atom of S facilitates near-unity intersystem crossing (k_{ISC})^{39,40} followed by triplet energy transfer from S to A (k_{TET}), TTA (γ_{TTA}), and electron injection from the upconverted singlet state of A ($k_{inj}(^1A^*)$). The rate constants and efficiencies for each of these processes were determined using comparative steady-state and time-resolved emission/absorption measurements following

our previously published procedure.^{31,36,41} For energy-transfer measurements, ZrO₂ instead of TiO₂ is used as a substrate because its relatively high conduction band (>2.0 V vs NHE) hinders excited-state electron transfer, and therefore, photo-physical events can be quantified in the absence of electron injection.⁴² The results are shown in Figure 4, and the experimental details are provided in the Supporting Information. The fast ($k_{ET_1} > 2.9 \times 10^{-9} s^{-1}$) and near-unity SS-to-S energy-transfer efficiency can be attributed to a combination of the spatial proximity and strong spectral overlap between the absorption of S and the emission of SS (Figure S1).^{31,43} Following intersystem crossing, $^3S^*$ to SS, nonproductive back triplet energy transfer was negligible as the $^3SS^*$ state was not observed by transient absorption (Figure S6) presumably because it is energetically uphill by ~ 200 mV,⁴⁴ making $k_{bET_1} \approx 0$. Similarly, following TTA-UC, fast $^1A^*$ -to-SS energy transfer ($k_{bET_2} = 4.4 \times 10^{-9} s^{-1}$) would be a major quenching pathway for UC emission. However, because electron injection from $^1A^*$ into TiO₂ ($k_{inj} > 4.5 \times 10^{11} s^{-1}$)⁴¹ is much faster than k_{bET_2} , energy losses via this pathway are negligible in the solar cell.

The J_{sc} of a device is proportional to the efficiency of electron injection, dye regeneration, charge collection, and light harvesting ($LHE(\lambda)$).⁴ Assuming that only $LHE(\lambda)$ is altered by the addition of SS, the theoretical photocurrent enhancement with singlet sensitization (J_{sc-SS}) relative to the bilayer device (J_{sc-bl}) can be calculated using

$$J_{sc-SS} = J_{sc-bl} \cdot Q \quad (1)$$

where Q is the gain factor determined by

$$Q = \frac{\%A_{tl}}{\%A_{bl}} \cdot M \cdot \frac{1}{1 - N} \quad (2)$$

where $\%A_{bl}$ and $\%A_{tl}$ are the integrated areas of the absorptance spectra from 455 to 535 nm for the bilayer and trilayer, respectively. M is the productive contribution from SS ($\Phi_{ET_1} \cdot (1 - \Phi_{bET_1}) \cdot (1 - \Phi_{bET_2})$), and N ($\Phi_{ET_1} \cdot (1 - \Phi_{bET_1}) \cdot \Phi_{bET_2}$) represents losses due to filtering/reabsorption by SS (details are provided in the Supporting Information). Given that $\Phi_{ET_1} \approx 100\%$ and Φ_{bET_1} is negligible, J_{sc-SS} was calculated to be $327 \mu A$ cm^{-2} , which is in reasonably good agreement with the experimentally determined $314 \pm 24 \mu A$ cm^{-2} . There was also similar agreement between calculated (1.2×10^{-15} excitation s^{-1} cm^{-1}) and experimental (1.3×10^{-15} excitation s^{-1} cm^{-1}) I_{th} values (details are provided in the Supporting Information). Collectively these results indicate that SS improves the TTA-UC solar cell performance by increasing photon absorption and funneling excited-state energy into the S-A UC process with negligible deleterious effects.

In conclusion, we have incorporated singlet sensitization into an integrated TTA-UC solar cell via self-assembled trilayers. This four-component photoanode (TiO₂, A, S, and SS) plus redox mediator is arguably the most complex, structured, energy and electron management scheme generated by humans to date. It facilitates directional SS-to-S singlet energy transfer and S-to-A triplet energy transfer, as well as cross surface energy migration, TTA, excited-state electron transfer from $^1A^*$ to TiO₂ followed by dye regeneration by a redox mediator in solution. The increased absorption

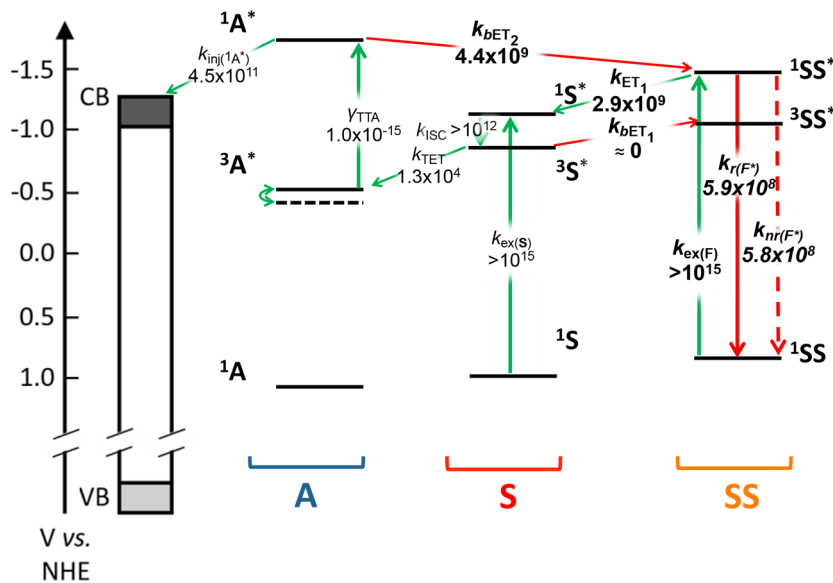


Figure 4. Productive (green) and nonproductive (red) dynamic events that occur in the $\text{TiO}_2\text{-A-S-SS}$ trilayer with their associated experimentally determined rate constants (all units in s^{-1} , except γ_{TTA} which is in $\text{cm}^3 \text{s}^{-1}$).

combined with directional energy transfer results in the highest reported TTA-UC photocurrent yet achieved under solar irradiance. These results demonstrated that singlet sensitization-enhanced self-assembled trilayers are a promising strategy for enhancing broad-band light absorption and improving the performance of TTA-UC solar cells. Increasing the absorptance (e.g., increased SS concentration or extinction coefficient) will be critical for realizing the full potential of the singlet sensitization scheme. However, it is important to note that in addition to increased absorptance, the system must retain high SS-to-S energy-transfer yields and SS should not inhibit dye regeneration by the redox mediator.

EXPERIMENTAL METHODS

Sample Preparation: Cell Fabrication. DSSCs were prepared similarly to our previously published procedure for electrochemical cells.^{27,28} Briefly, FTO glass was cut into $2 \text{ cm} \times 2.5 \text{ cm}$ pieces, and an active area of 1 cm^2 metal oxide was prepared by doctor blading TiO_2 (1 layer of Scotch tape) and sintering.⁴⁵ Dyes were then loaded onto the metal oxide as described below. To generate the counter electrode, a small hole ($d = 1.1 \text{ mm}$) was drilled into the corner of the $2 \text{ cm} \times 2.5 \text{ cm}$ glass slide, and then H_2PtCl_6 solution ($50 \mu\text{L}$, 5 mM in ethanol) was drop-cast onto the slide that was then heat-dried at 400°C for 20 min. A 2 mm wide $2 \text{ cm} \times 2 \text{ cm}$ Meltonix film was placed between the two glass slides, and the entire ensembles were heated to $\sim 150^\circ\text{C}$ for 7 s using a home-built heating/sealing device described previously.⁴⁶ The cells were then transferred to a glovebox (VTI Universal purified glovebox, N_2 atmosphere) where the $\text{Co}^{\text{II}}/\text{Co}^{\text{III}}(\text{phen})_3$ mediator electrolyte, dissolved in dry and oxygen-free MeCN, was injected using a Vac'n Fill Syringe through the 1.1 mm diameter hole. A Meltonix film and small piece of a micro glass cover slide were then heated to seal the hole used for electrolyte injection.

Samples for emission measurements were prepared in a similar fashion. Briefly, glass was cut into $2.2 \text{ cm} \times 2.2 \text{ cm}$ pieces, and an active area of 1 cm^2 metal oxide was prepared by doctor blading ZrO_2 (1 layer Scotch tape) and sintering. A

small hole was drilled into the corner of the $2.2 \text{ cm} \times 2.2 \text{ cm}$ glass slide. A 2 mm wide $2.2 \text{ cm} \times 2.2 \text{ cm}$ Meltonix film was placed between the two glass slides and then assembled. Dry and oxygen-free MeCN was injected to fill the interior of the cells in the glovebox, and then the cells were sealed with Meltonix film and a micro glass cover.

Dye Loading. The TiO_2 films on FTO glass were functionalized with monolayer of A or B by soaking in their respective loading solutions of A in DMSO ($200 \mu\text{M}$) and B in DMSO ($400 \mu\text{M}$) for 12 h. The $\text{TiO}_2\text{-A/B}$ films were then soaked in a loading solution of $\text{Zn}(\text{CH}_3\text{COO})_2$ in MeOH ($400 \mu\text{M}$) for 2 h, followed by a $200 \mu\text{M}$ S solution of DMSO for 2 h with N_2 bubbling, resulting in $\text{TiO}_2\text{-A/B-S}$. $\text{TiO}_2\text{-A-S-SS}$ was achieved by soaking $\text{TiO}_2\text{-A-S}$ for 12 h in Zn loading solution then $300 \mu\text{M}$ SS solution of MeOH for 30 min. The ZrO_2 film on glass was prepared by the same stepwise soaking method.

Surface Coverages. In accord with our previously published procedure,²⁸ surface coverages (Γ in mol cm^{-2}) are estimated with the expression $\Gamma = (A(\lambda)/\varepsilon(\lambda))/1000$, where ε is the molar extinction coefficient of A and S in DMSO²⁷ and SS in MeOH (Table S3) and $A(\lambda)$ is the absorbance of each component on the fully loaded slides.

ASSOCIATED CONTENT

Supporting Information

The Supporting Information is available free of charge on the ACS Publications website at DOI: [10.1021/acsenergylett.9b00870](https://doi.org/10.1021/acsenergylett.9b00870).

Experimental details, energy level calculation, theoretical I_{th} calculation, photophysical properties of SS, device measurement data, and transient absorption spectra (PDF)

AUTHOR INFORMATION

Corresponding Author

*E-mail: hanson@chem.fsu.edu. Web: <https://www.chem.fsu.edu/~hanson/>. Twitter: @HansonFSU.

ORCID 

Yan Zhou: [0000-0002-7290-1401](https://orcid.org/0000-0002-7290-1401)

Kenneth Hanson: 0000-0001-7219-7808

Author Contributions

[‡]Y.Z. and C.R. contributed equally.

Notes

The authors declare no competing financial interest.

ACKNOWLEDGMENTS

This material is based upon work supported by the National Science Foundation under Grant No. DMR-1752782 and CHE-1531629. We thank Peter I. Djurovich for his valuable insights.

REFERENCES

- (1) Hohmann-Marriott, M. F.; Blankenship, R. E. Evolution of Photosynthesis. *Annu. Rev. Plant Biol.* **2011**, *62* (1), 515–548.
- (2) Miyasaka, H. Control of Charge Transfer in Donor/Acceptor Metal–Organic Frameworks. *Acc. Chem. Res.* **2013**, *46* (2), 248–257.
- (3) Smith, M. B.; Michl, J. Singlet Fission. *Chem. Rev.* **2010**, *110* (11), 6891–6936.
- (4) Wang, J. C.; Hill, S. P.; Dilbeck, T.; Ogunsolu, O. O.; Banerjee, T.; Hanson, K. Multimolecular assemblies on high surface area metal oxides and their role in interfacial energy and electron transfer. *Chem. Soc. Rev.* **2018**, *47* (1), 104–148.
- (5) Terada, K.; Kobayashi, K.; Hikita, J.; Haga, M.-a. Electric Conduction Properties of Self-assembled Monolayer Films of Ru Complexes with Disulfide/Phosphonate Anchors in a Au–(Molecular Ensemble)–(Au Nanoparticle) Junction. *Chem. Lett.* **2009**, *38* (5), 416–417.
- (6) Lee, H.; Kepley, L. J.; Hong, H. G.; Mallouk, T. E. Inorganic analogs of Langmuir–Blodgett films: adsorption of ordered zirconium 1,10-decanebisphosphonate multilayers on silicon surfaces. *J. Am. Chem. Soc.* **1988**, *110* (2), 618–620.
- (7) Caulder, D. L.; Raymond, K. N. Supermolecules by Design. *Acc. Chem. Res.* **1999**, *32* (11), 975–982.
- (8) Lehn, J. M. *Supramolecular Chemistry: Concepts and Perspectives*; Wiley-VCH: Weinheim, 2006.
- (9) Yanai, N.; Kimizuka, N. Recent emergence of photon upconversion based on triplet energy migration in molecular assemblies. *Chem. Commun.* **2016**, *52* (31), 5354–5370.
- (10) Gray, V.; Moth-Poulsen, K.; Albinsson, B.; Abrahamsson, M. Towards efficient solid-state triplet–triplet annihilation based photon upconversion: Supramolecular, macromolecular and self-assembled systems. *Coord. Chem. Rev.* **2018**, *362*, 54–71.
- (11) Singh-Rachford, T. N.; Castellano, F. N. Photon upconversion based on sensitized triplet–triplet annihilation. *Coord. Chem. Rev.* **2010**, *254* (21), 2560–2573.
- (12) Shockley, W.; Queisser, H. J. Detailed Balance Limit of Efficiency of p-n Junction Solar Cells. *J. Appl. Phys.* **1961**, *32* (3), 510–519.
- (13) Ekins-Daukes, N. J.; Schmidt, T. W. A molecular approach to the intermediate band solar cell: The symmetric case. *Appl. Phys. Lett.* **2008**, *93* (6), No. 063507.
- (14) Schulze, T. F.; Schmidt, T. W. Photochemical upconversion: present status and prospects for its application to solar energy conversion. *Energy Environ. Sci.* **2015**, *8* (1), 103–125.
- (15) Cheng, Y. Y.; Fuckel, B.; MacQueen, R. W.; Khoury, T.; Clady, R. G. C. R.; Schulze, T. F.; Ekins-Daukes, N. J.; Crossley, M. J.; Stannowski, B.; Lips, K.; Schmidt, T. W. Improving the light-harvesting of amorphous silicon solar cells with photochemical upconversion. *Energy Environ. Sci.* **2012**, *5* (5), 6953–6959.
- (16) Schulze, T. F.; Czolk, J.; Cheng, Y.-Y.; Fuckel, B.; MacQueen, R. W.; Khoury, T.; Crossley, M. J.; Stannowski, B.; Lips, K.; Lemmer, U.; Colsmann, A.; Schmidt, T. W. Efficiency Enhancement of Organic and Thin-Film Silicon Solar Cells with Photochemical Upconversion. *J. Phys. Chem. C* **2012**, *116* (43), 22794–22801.
- (17) Monguzzi, A.; Borisov, S. M.; Pedrini, J.; Klimant, I.; Salvalaggio, M.; Biagini, P.; Melchiorre, F.; Lelii, C.; Meinardi, F. Efficient Broadband Triplet–Triplet Annihilation-Assisted Photon Upconversion at Subsolar Irradiance in Fully Organic Systems. *Adv. Funct. Mater.* **2015**, *25* (35), 5617–5624.
- (18) Nattestad, A.; Cheng, Y. Y.; MacQueen, R. W.; Schulze, T. F.; Thompson, F. W.; Mozer, A. J.; Fuckel, B.; Khouri, T.; Crossley, M. J.; Lips, K.; Wallace, G. G.; Schmidt, T. W. Dye-Sensitized Solar Cell with Integrated Triplet–Triplet Annihilation Upconversion System. *J. Phys. Chem. Lett.* **2013**, *4* (12), 2073–2078.
- (19) Ahmad, S.; Liu, J.; Gong, C.; Zhao, J.; Sun, L. Photon Upconversion via Epitaxial Surface-Supported Metal–Organic Framework Thin Films with Enhanced Photocurrent. *ACS Appl. Energy Mater.* **2018**, *1* (2), 249–253.
- (20) Lin, Y. L.; Koch, M.; Brigeman, A. N.; Freeman, D. M. E.; Zhao, L.; Bronstein, H.; Giebink, N. C.; Scholes, G. D.; Rand, B. P. Enhanced sub-bandgap efficiency of a solid-state organic intermediate band solar cell using triplet-triplet annihilation. *Energy Environ. Sci.* **2017**, *10* (6), 1465–1475.
- (21) Frazer, L.; Gallaher, J. K.; Schmidt, T. W. Optimizing the Efficiency of Solar Photon Upconversion. *ACS Energy Lett.* **2017**, *2* (6), 1346–1354.
- (22) Monguzzi, A.; Oertel, A.; Braga, D.; Riedinger, A.; Kim, D. K.; Knuessel, P. N.; Bianchi, A.; Mauri, M.; Simonutti, R.; Norris, D. J.; Meinardi, F. Photocatalytic Water-Splitting Enhancement by Sub-Bandgap Photon Harvesting. *ACS Appl. Mater. Interfaces* **2017**, *9* (46), 40180–40186.
- (23) Choi, D.; Nam, S. K.; Kim, K.; Moon, J. H. Enhanced Photoelectrochemical Water Splitting through Bismuth Vanadate with a Photon Upconversion Luminescent Reflector. *Angew. Chem., Int. Ed.* **2019**, *58*, 6891.
- (24) Zhou, J.; Liu, Q.; Feng, W.; Sun, Y.; Li, F. Upconversion Luminescent Materials: Advances and Applications. *Chem. Rev.* **2015**, *115* (1), 395–465.
- (25) Lissau, J. S.; Gardner, J. M.; Morandeira, A. Photon Upconversion on Dye-Sensitized Nanostructured ZrO₂ Films. *J. Phys. Chem. C* **2011**, *115* (46), 23226–23232.
- (26) Simpson, C.; Clarke, T. M.; MacQueen, R. W.; Cheng, Y. Y.; Trevitt, A. J.; Mozer, A. J.; Wagner, P.; Schmidt, T. W.; Nattestad, A. An intermediate band dye-sensitized solar cell using triplet-triplet annihilation. *Phys. Chem. Chem. Phys.* **2015**, *17* (38), 24826–24830.
- (27) Hill, S. P.; Banerjee, T.; Dilbeck, T.; Hanson, K. Photon Upconversion and Photocurrent Generation via Self-Assembly at Organic–Inorganic Interfaces. *J. Phys. Chem. Lett.* **2015**, *6* (22), 4510–4517.
- (28) Hill, S. P.; Dilbeck, T.; Baduell, E.; Hanson, K. Integrated Photon Upconversion Solar Cell via Molecular Self-Assembled Bilayers. *ACS. Energy. Lett.* **2016**, *1* (1), 3–8.
- (29) Dilbeck, T.; Hill, S. P.; Hanson, K. Harnessing molecular photon upconversion at sub-solar irradiance using dual sensitized self-assembled trilayers. *J. Mater. Chem. A* **2017**, *5* (23), 11652–11660.
- (30) Zhou, Y.; Hill, S. P.; Hanson, K. Influence of meta- and para-phosphonated diphenylanthracene on photon upconversion in self-assembled bilayers. *J. Photonics Energy* **2018**, *8* (11), 1–11.
- (31) Zhou, Y.; Ayad, S.; Ruchlin, C.; Posey, V.; Hill, S. P.; Wu, Q.; Hanson, K. Examining the Role of Acceptor Molecule Structure in Self-Assembled Bilayers: Surface Loading, Stability, Energy Transfer, and Upconverted Emission. *Phys. Chem. Chem. Phys.* **2018**, *20* (31), 20513–20524.
- (32) Hill, S. P.; Hanson, K. Harnessing Molecular Photon Upconversion in a Solar Cell at Sub-solar Irradiance: Role of the Redox Mediator. *J. Am. Chem. Soc.* **2017**, *139* (32), 10988–10991.
- (33) Dilbeck, T.; Hanson, K. Molecular Photon Upconversion Solar Cells Using Multilayer Assemblies: Progress and Prospects. *J. Phys. Chem. Lett.* **2018**, *9* (19), 5810–5821.
- (34) Pedrini, J.; Monguzzi, A.; Meinardi, F. Cascade sensitization of triplet–triplet annihilation based photon upconversion at sub-solar irradiance. *Phys. Chem. Chem. Phys.* **2018**, *20* (15), 9745–9750.
- (35) Hanson, K.; Torelli, D. A.; Vannucci, A. K.; Brennaman, M. K.; Luo, H.; Alibabaei, L.; Song, W.; Ashford, D. L.; Norris, M. R.; Glasson, C. R. K.; Concepcion, J. J.; Meyer, T. J. Self-Assembled

Bilayer Films of Ruthenium(II)/Polypyridyl Complexes through Layer-by-Layer Deposition on Nanostructured Metal Oxides. *Angew. Chem., Int. Ed.* **2012**, *51* (51), 12782–12785.

(36) Wang, J. C.; Murphy, I. A.; Hanson, K. Modulating Electron Transfer Dynamics at Dye–Semiconductor Interfaces via Self-Assembled Bilayers. *J. Phys. Chem. C* **2015**, *119* (7), 3502–3508.

(37) Monguzzi, A.; Mezyk, J.; Scotognella, F.; Tubino, R.; Meinardi, F. Upconversion-induced fluorescence in multicomponent systems: Steady-state excitation power threshold. *Phys. Rev. B: Condens. Matter Mater. Phys.* **2008**, *78* (19), 195112.

(38) Haefele, A.; Blumhoff, J.; Khnayzer, R. S.; Castellano, F. N. Getting to the (Square) Root of the Problem: How to Make Noncoherent Pumped Upconversion Linear. *J. Phys. Chem. Lett.* **2012**, *3* (3), 299–303.

(39) Kim, D.; Holten, D.; Gouterman, M.; Buchler, J. W. Comparative photophysics of platinum(II) and platinum(IV) porphyrins. *J. Am. Chem. Soc.* **1984**, *106* (14), 4015–4017.

(40) Eastwood, D.; Gouterman, M. Porphyrins: XVIII. Luminescence of (Co), (Ni), Pd, Pt complexes. *J. Mol. Spectrosc.* **1970**, *35* (3), 359–375.

(41) Dilbeck, T.; Wang, J. C.; Zhou, Y.; Olsson, A.; Sykora, M.; Hanson, K. Elucidating the Energy- and Electron-Transfer Dynamics of Photon Upconversion in Self-Assembled Bilayers. *J. Phys. Chem. C* **2017**, *121* (36), 19690–19698.

(42) Katoh, R.; Furube, A.; Yoshihara, T.; Hara, K.; Fujihashi, G.; Takano, S.; Murata, S.; Arakawa, H.; Tachiya, M. Efficiencies of Electron Injection from Excited N3 Dye into Nanocrystalline Semiconductor (ZrO₂, TiO₂, ZnO, Nb₂O₅, SnO₂, In₂O₃) Films. *J. Phys. Chem. B* **2004**, *108* (15), 4818–4822.

(43) Giribabu, L.; Ashok Kumar, A.; Neeraja, V.; Maiya, B. G. Orientation Dependence of Energy Transfer in an Anthracene–Porphyrin Donor–Acceptor System. *Angew. Chem.* **2001**, *113* (19), 3733–3736.

(44) Song, L.; Varma, C. A.; Verhoeven, J. W.; Tanke, H. J. Influence of the triplet excited state on the photobleaching kinetics of fluorescein in microscopy. *Biophys. J.* **1996**, *70* (6), 2959–2968.

(45) Song, W.; Glasson, C. R. K.; Luo, H.; Hanson, K.; Brennaman, M. K.; Concepcion, J. J.; Meyer, T. J. Photoinduced Stepwise Oxidative Activation of a Chromophore–Catalyst Assembly on TiO₂. *J. Phys. Chem. Lett.* **2011**, *2* (14), 1808–1813.

(46) Ogunsolu, O. O.; Murphy, I. A.; Wang, J. C.; Das, A.; Hanson, K. Energy and Electron Transfer Cascade in Self-Assembled Bilayer Dye-Sensitized Solar Cells. *ACS Appl. Mater. Interfaces* **2016**, *8* (42), 28633–28640.